energies

Article

Multiobjective Optimization for a Li-Ion Battery and Supercapacitor Hybrid Energy Storage Electric Vehicle

Gang Xiao [1,2], Qihong Chen [1], Peng Xiao [1,*], Liyan Zhang [1] and Quansen Rong [1]

1 School of Automation, Wuhan University of Technology, Wuhan 430070, China; 290401@whut.edu.cn (G.X.); chenqh@whut.edu.cn (Q.C.); zlywhut@whut.edu.cn (L.Z.); 302825@whut.edu.cn (Q.R.)
2 Wuhan Digital Engineering Institute, Wuhan 430074, China
* Correspondence: xp@whut.edu.cn

Abstract: The acceptance of hybrid energy storage system (HESS) Electric vehicles (EVs) is increasing rapidly because they produce zero emissions and have a higher energy efficiency. Due to the nonlinear and strong coupling relationships between the sizing parameters of the HESS components and the control strategy parameters and EV's performances, energy consumption rate, running range and HESS cost, how to design the HESS EVs for different preferences is a key problem. How to get the real time performances from the HESS EV is a difficulty. The multiobjective optimization for the HESS EV considering the real time performances and the HESS cost is a solution. A Li-ion battery (*BT*) semi-active HESS and optimal energy control strategy were proposed for an EV. The multiobjectives include energy consumption over 100 km, acceleration time from 0–100 km per hour, maximum speed, running range and HESS cost of the EV. According to the degrees of impact on the multiobjectives, the scaled factors of *BT* capacity, the series number of Li-ion *BT*s, the series number of super-capacitors (SCs), the parallel number of SCs, and charge power of the SCs were chosen as the optimization variables. Two sets of different weights were used to simulate the multiobjective optimization problem in the ADVISOR software linked with MATLAB software. The simulation results show that some of the multiobjectives are sensitive to their weights. HESS EVs meeting different preferences can be designed through the weights of different objectives. Compared with the direct optimization algorithm, the genetic algorithm (GA) has a stronger optimization ability, and the single objective is more sensitive to its corresponding weight. The proposed optimization method is practical for a Li-ion *BT* and SC HESS EV design.

Keywords: multiobjective optimization; genetic algorithm; battery; supercapacitor; hybrid energy storage system; electric vehicle

check for updates

Citation: Xiao, G.; Chen, Q.; Xiao, P.; Zhang, L.; Rong, Q. Multiobjective Optimization for a Li-Ion Battery and Supercapacitor Hybrid Energy Storage Electric Vehicle. *Energies* **2022**, *15*, 2821. https://doi.org/10.3390/en15082821

Academic Editor: Xi Li

Received: 4 March 2022
Accepted: 10 April 2022
Published: 12 April 2022

1. Introduction

Due to advantages such as energy conservation, environmental protection, and low charging cost, EVs have been gradually accepted by the market [1,2]. EVs have been considered as a good approach to reduce carbon dioxide emissions, for EVs can overcome the shortcomings of traditional fuel vehicle exhaust pollution. At the same time, EVs can save energy because they can be charged when the power consumption of the power grid is low [3]. The *BT* is one of the most expensive components of the EV and has a decisive impact on EV's price and some of their performance [4]. In current EVs, the *BT*s are always oversized in order to improve power performance and acceleration capability. Such challenges as power performance, running range, lifetime of the *BT*, and cost of the EV with a sole energy storage system limit the EV's wider use.

The SC has the advantages of high-power density, short charge and discharge time, and long service life and is less affected by the temperature, but the energy density is small [5]. The Li-ion *BT* and SC HESS can make up for the advantages of both sides while avoiding their disadvantages [6].

The *BT* and SC HESS is widely used in different objects and occasions. The *BT* and SC HESS in smart phones extends the service life of Li-ion BTs [7]. The lead-acid *BT* and SC HESS in trucks reduces carbon dioxide emissions [8–10]. The *BT* and SC HESS reduces the power fluctuation of fuel cell and wind energy in the HESS with fuel cell and wind energy [11–16].

The performance of *BT* and SC HESS depends on an appropriate energy management strategy. The wavelet analysis method is used to identify the road conditions; then, the neural network is used to learn the conditions data, and the fuzzy energy management strategy is used to distribute the power of the HESS, which improves vehicle performance [17]. The HESS real-time energy management strategy based on SC voltage detection has achieved good results. By improving the topology of HESS, flexible control of lithium *BT* current is realized, and the effect of energy management is improved. The power performance of HESS is improved by the fuzzy predictive control method [18]. A HESS energy management strategy based on dynamic programming considering lithium *BT* degradation is proposed [19].

Compared with the *BT*, the HESS not only improves the performance but also leads to the increase of system complexity and cost. Therefore, the evaluation and optimization of HESS should be carried out with multiple objectives. The purpose of HESS EV is to improve the performances of the EV while taking into account the economy of the EV.

The GA algorithm is widely used in the field of EV optimization [20–24]. The GA algorithm is used to optimize the multi objectives of fuel cell current, lithium *BT* current, lithium *BT*'s *SOC* change, SC's *SOC* change, and hydrogen consumption cost by the control of the powers of the *BT* and SC and the load in the fuel cell, *BT*, and SC hybrid EV [20]. The multi-objective GA algorithm is used to optimize the automotive electric transmission [21]. The GA algorithm is used to optimize the location and power of EV charging stations [22,23]. The multi-objective GA algorithm is used to optimize the driving paths and powers of multi depot vehicle [24].

The above studies focus on comparing HESS performance with *BT* or SC performance or, for specific HESS, using an intelligent control method to optimize the energy management strategy and improve the HESS performance, with less consideration of the influence of the sizing parameters of components in HESS and less consideration of the optimal design based on the EV's specific performance indicators in the optimization. At the same time, how to get the real time performances of the HESS EV is a difficulty. In this paper, a multiobjective optimization on a *BT* and SC HESS EV using both GA algorithm and ADVISOR software will be studied. The real time performances of the HESS EV are obtained by the ADVISOR software. The EV's energy consumption over 100 km, acceleration time from 0–100 km per hour, maximum speed, HESS cost, and running range are considered in the objective function. The structure of the paper is as follows: The fundamentals of a *BT* semi-active HESS EV, the scheme of the multiobjective optimization and an optimal energy management strategy are designed in Section 2. Section 3 focuses on the multiobjective problem analysis. In Section 4 the GA algorithm optimization based on ADVISOR software and MATLAB software is carried out. The study discussion is also presented in Section 4. The conclusions are presented in Section 5.

2. Fundamentals of a BT Semi-Active HESS

2.1. HESS Components

ADVISOR software is a popular advanced vehicle simulation software, which is especially suitable for vehicle performance evaluation, testing, and optimization. A variety of vehicle structures such as traditional fuel vehicles, pure EVs, and fuel cell and Li-ion BT hybrid vehicles are available in the ADVISOR software, but there is no *BT* and SC HESS EV model available [25]. The new *BT*'s semi-active HESS EV model is specially developed in the ADVISOR software. The semi-active HESS architecture is reasonable for EVs considering the HESS cost, efficiency, and reliability. The *BT*'s semi-active HESS structure is easy to lead to unstable motor voltage, but it is still within a range of voltage fluctuation that the motor can withstand. The Li-ion *BT* pack is connected to the input of the motor controller through a DC/DC converter, and the SC pack is directly connected to the input of the motor controller. The *BT* semi-active HESS scheme in the ADVISOR software is shown in Figure 1.

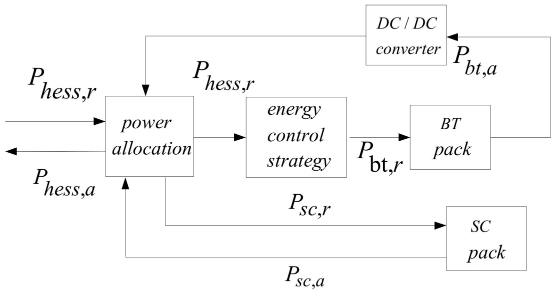

Figure 1. A *BT* semi-active HESS scheme in the ADVISOR software.

The SC pack consists of $N_{sc,p}$ strings in parallel and $N_{sc,s}$ SCs in series. The *BT* pack consists of $N_{bt,s}$ *BT*s in series. $P_{hess,r}$ is the required power of the HESS. $P_{hess,a}$ is the available output power of the HESS. $P_{bt,r}$ is the required power of the Li-ion *BT* pack. $P_{bt,a}$ is the available output power of the Li-ion *BT* pack. $P_{sc,r}$ is the power required of the SC pack. $P_{sc,a}$ is the available output power of the SC pack.

A midsize EV's parameters are listed in Table 1. A Saft VL45E $LiFePO_4$ *BT* is used, whose parameters are listed in Table 2 [25]. A Maxwell BACP3000 SC is chosen for the HESS, whose parameters are listed in Table 3 [25]. A Westinghouse AC75 motor model is used with the parameters listedin Table 4 [26].

Table 1. EV's model parameters.

Parameters	Value
Cargo mass/kg	200
Glider mass/kg	680
Wheelbase/m	2.7
Frontal area/m^2	2.6

Table 2. SAFT VL45E Li-ion BT parameters.

Parameters	Value
Capacity/Ah	44
Internal resistance/mΩ	3.6
Stored energy/Wh	140
Mass/kg	0.91

Table 3. BACP3000 SC parameters.

Parameters	Value
Rated capacitance/F	3000
Internal resistance/mΩ	0.29
Stored energy/Wh	3.04
Mass/kg	0.51
Usable power/W·kg^{-1}	5900

Table 4. Motor parameters.

Parameters	Value
Max. power/kW	75
Max. voltage/V	375
Min. voltage/V	120

2.2. The Scheme of the Multiobjective Optimization for the HESS EV

The scheme of the multiobjective optimization for the HESS EV is as in Figure 2. The optimal energy control strategy of the HESS will be designed in the HESS EV in the ADVISOR software by secondary development at first. Then, the relationships between the sizing parameters of the HESS components and the control strategy parameters and EV's real time performances, energy consumption rate, running range and HESS cost, etc., can be obtained by the HESS EV performance simulation in the ADVISOR software. According to the degrees of impacts between them, the optimization variables and multiobjects are selected. Then, a multiobjective optimization in the ADVISOR software linked with the MATLAB software can be carried out with two sets of weights. The conclusion and discussion will be presented at the end.

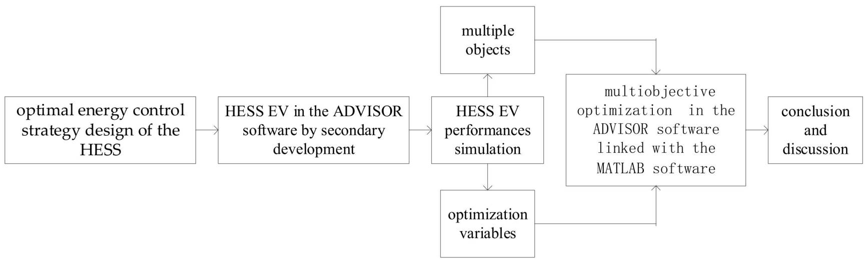

Figure 2. The scheme of the multiobjective optimization for the HESS EV.

2.3. The Optimal Energy Control Strategy of the HESS

An optimal energy control strategy is proposed for the *BT* semi-active HESS. The optimal energy control strategy distributes the output powers of *BT* and SC according to the required power of the HESS and the *SOC* of the SC pack. The available output power of the Li-ion *BT* pack is limited within the rated value of high efficiency to extend the life of the *BT*, but the available output power of the SC pack can fluctuate greatly for the good performance of the SC pack. The power fluctuation of the EV is large and frequent, and therefore, the SC pack is used as an energy buffer. The SC pack adopts the charge sustaining energy management strategy to meet the power demand of the HESS and maintain the state of charge (*SOC*) of the SC pack near the target value as far as possible. The optimal control strategy is shown in Figure 3.

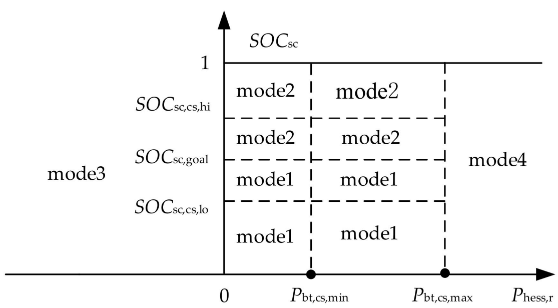

Figure 3. Optimal energy control strategy.

SOC_{sc} is the SOC of the SC pack. $SOC_{sc,cs,hi}$ is the high SOC of the SC pack. $SOC_{sc,cs,lo}$ is the low SOC of the SC pack. $SOC_{sc,goal}$ is the goal value of SOC_{sc}. The optimal control strategy works on the following rules:

(a) In normal cases, in order to improve the efficiency and service life of lithium BT, $P_{bt,r}$ is limited by the minimum control power $P_{bt,cs,min}$ and the maximum control power $P_{bt,cs,max}$.
(b) When $P_{hess,r} \in [0, P_{bt,cs,max}]$ and $SOC_{sc} \in [0, SOC_{sc,goal}]$, as the mode 1 in Figure 3, the SC pack is charged by the BT pack, and SOC_{sc} approaches $SOC_{sc,goal}$.
(c) When $P_{hess,r} \geq P_{bt,cs,max}$, as the mode 4 in Figure 3, both the BT pack and SC pack provide power to the EV.
(d) When $P_{hess,r} \in [0, P_{bt,cs,max}]$ and $SOC_{sc} \in [SOC_{sc,goal}, 1]$, as the mode 2 in Figure 3, the SC pack discharges, and SOC_{sc} approaches $SOC_{sc,goal}$.
(e) When $P_{hess,r} \leq 0$, as the mode 3 in Figure 3, the SC pack recovers all regenerative braking power.

When $P_{hess,r} \leq 0$, $P_{bt,r}$ is shown in Equation (1).

$$P_{bt,r} = P_{bt,cs,min} \tag{1}$$

When $P_{hess,r} > 0$, $P_{bt,r}$ is shown in Equation (2).

$$P_{bt,r} = P_{hess,r} + P_{additional} \tag{2}$$

$E_{sc,cs,hi}$ is the energy of the SC pack when SOC_{sc} is $SOC_{sc,cs,hi}$. $E_{sc,cs,lo}$ is the energy of the SC pack when SOC_{sc} is $SOC_{sc,cs,lo}$. $E_{sc,goal}$ is the energy of the SC pack when SOC_{sc} is $SOC_{sc,goal}$. $E_{sc,goal}$ is the average value of $E_{sc,cs,hi}$ and $E_{sc,cs,lo}$, as in Equation (3).

$$E_{sc,goal} = 0.5 \times (E_{sc,cs,hi} + E_{sc,cs,lo}) \tag{3}$$

According to the SC's energy formula, $E_{sc,goal}$ and $E_{sc,cs,hi}$, $E_{sc,cs,lo}$ are as in Equations (4)–(6), respectively.

$$E_{sc,goal} = 0.5 \times C \times V^2{}_{sc,goal} = 0.5 \times C \times V^2 \times SOC^2{}_{sc,goal} \tag{4}$$

$$E_{sc,cs,hi} = 0.5 \times C \times V^2{}_{sc,cs,hi} = 0.5 \times C \times V^2 \times SOC^2{}_{sc,cs,hi} \tag{5}$$

$$E_{sc,cs,lo} = 0.5 \times C \times V^2{}_{sc,cs,lo} = 0.5 \times C \times V^2 \times SOC^2{}_{sc,cs,lo} \tag{6}$$

C is the SC's capacitance; V is the SC's voltage. $SOC_{sc,goal}$ is obtained from Equations (3)–(6), which is shown in Equation (7).

$$SOC_{sc,goal} = \sqrt{\frac{SOC^2{}_{sc,cs,hi} + SOC^2{}_{sc,cs,lo}}{2}} \tag{7}$$

$P_{additional}$ is the additional power needed to maintain SOC_{sc} near $SOC_{sc,goal}$. $P_{additional}$ is shown in Equation (8).

$$P_{additional} = \frac{SOC_{sc,goal} - SOC_{sc}}{0.5 \times (SOC_{sc,cs,hi} - SOC_{sc,cs,lo})} \cdot P_{charge} \tag{8}$$

P_{charge} is the charge power of the SC pack.
$P_{sc,r}$ is as shown in Equation (9).

$$P_{sc,r} = P_{hess,r} - P_{bt,a} \cdot \eta_{DC/DC} \tag{9}$$

$\eta_{DC/DC}$ is energy conversion efficiency of the DC/DC converter.
The parameters of the optimal energy control strategy are in Table 5.

Table 5. The optimal energy control strategy parameters.

Parameters	Value
$P_{\text{bt,cs,min}}/\text{kW}$	1.5
$P_{\text{bt,cs,max}}/\text{kW}$	12
$\eta_{\text{DC/DC}}$	0.95
$SOC_{\text{sc,init}}$	0.9
$SOC_{\text{sc,goal}}$	0.74
$SOC_{\text{sc,cs,hi}}$	0.95
$SOC_{\text{sc,cs,lo}}$	0.45

$SOC_{\text{sc,init}}$ is the initial value of SOC_{sc}.

3. Multiobjective Optimization Analysis

The HESS EV performance simulation results [26] of the HESS EV in the ADVISOR software show that both the sizing parameters of the HESS components and the control strategy parameters have a certain impact on EV's performances, energy consumption rate, running range, and HESS cost. When k_{bt} increases, t_{100}, Q_{100}, l, and C_{hess} increases, and $V_{\text{veh,max}}$ decreases. When $N_{\text{bt,s}}$ increases, $V_{\text{veh,max}}$, t_{100}, l, and C_{hess} increase, and Q_{100} increases or decreases. When $N_{\text{sc,s}}$ increases, $V_{\text{veh,max}}$, Q_{100}, and C_{hess} increase, and t_{100} and l decrease. When $N_{\text{sc,p}}$ increases, $V_{\text{veh,max}}$, l, and C_{hess} increase, and Q_{100} and t_{100} decrease. When P_{charge} increases, $V_{\text{veh,max}}$ and Q_{100} increase, and t_{100}, l and C_{hess} decrease. Therefore, the relationships between the sizing parameters of the HESS components and the control strategy parameters and EV's performances, energy consumption rate, running range, and the HESS cost are nonlinear and strong coupling.

The HESS EV performance simulation results show that, among the sizing parameters of HESS's components and the control strategy parameters, the scaled factors of BT capacity k_{bt}, $N_{\text{bt,s}}$, $N_{\text{sc,s}}$, $N_{\text{sc,p}}$, and P_{charge} have a greater impact on the five objectives, while other parameters have less impact on the five objectives. Therefore, k_{bt}, $N_{\text{bt,s}}$, $N_{\text{sc,s}}$, $N_{\text{sc,p}}$, and P_{charge} are selected as the optimization variables.

The semi-active HESS EV evaluation focuses on the energy consumption over 100 km Q_{100}, the acceleration time from 0–100 km per hour t_{100}, the maximum speed $V_{\text{veh,max}}$, the running range l, and the HESS cost C_{hess}, which are essentially contradictory. The variables of the multiobjective optimization problem for the HESS EV contain k_{bt}, $N_{\text{bt,s}}$, $N_{\text{sc,s}}$, $N_{\text{sc,p}}$, and P_{charge}, as shown in Equation (10).

$$f(x) = [k_{bt}, N_{bt,s}, N_{sc,p}, N_{\text{sc,s}}, P_{\text{charge}}] \tag{10}$$

The HESS EV performance simulation results and the HESS EV performance constraints reduce the amount of calculations during the optimization. The varied ranges of the variables are described in Equation (11).

$$x_1 \in [1,4], x_2 \in [50,\ 150], x_3 \in [1\text{–}4], x_4 \in [75,\ 135], x_5 \in [6000,\ 9000] \tag{11}$$

The multiobjective function is given by Equation (12). The optimization objective is to maximize the value of F(x).

$$F(x) = w_1 \cdot (1 - t_{100\cdot\text{norm}}) + w_2 \cdot V_{veh,max,\text{norm}} + w_3 \cdot l_{\text{norm}} + w_4 \cdot (1 - Q_{100\cdot\text{norm}}) + w_5 (1 - C_{\text{hess,norm}}) \tag{12}$$

$t_{100,\text{norm}}$,$V_{\text{veh,max,norm}}$, l_{norm}, $Q_{100,\text{norm}}$, and $C_{\text{hess,norm}}$ are the normalization value of t_{100}, $V_{\text{veh,max}}$, l, $Q_{100,}$ and C_{hess}, between zero and one, based on the maximum and minimum values obtained.

$t_{100,\text{norm}}$ is shown in Equation (13).

$$t_{100,norm} = \frac{t_{100} - t_{100,min}}{t_{100,max} - t_{100,min}} \tag{13}$$

$t_{100,\min}$ is the reference minimum value of t_{100}, and $t_{100,\max}$ is the reference maximum value of t_{100}.

$V_{\mathrm{veh,max,norm}}$ is shown in Equation (14).

$$V_{\mathrm{veh,max},norm} = \frac{V_{\mathrm{veh,max}} - V_{veh,max,min}}{V_{\mathrm{veh,max},max} - V_{veh,max,min}} \tag{14}$$

$V_{\mathrm{veh,max,min}}$ is the reference minimum value of $V_{\mathrm{veh,max}}$, and $V_{\mathrm{veh,max,max}}$ is the maximum value of $V_{\mathrm{veh,max}}$.

l_{norm} is shown in Equation (15).

$$l_{\mathrm{norm}} = \frac{l - l_{\min}}{l_{\max} - l_{\min}} \tag{15}$$

$l_{\min}$ is the reference minimum value of l, and $l_{\max}$ is the reference maximum value of l.

$Q_{100,\mathrm{norm}}$ is shown in Equation (16).

$$Q_{100,\mathrm{norm}} = \frac{Q_{100} - Q_{100,\min}}{Q_{100,\max} - Q_{100,\min}} \tag{16}$$

$Q_{100,\min}$ is the reference minimum value of Q_{100}, and $Q_{100,\max}$ is the reference maximum value of Q_{100}.

$C_{\mathrm{hess,norm}}$ is shown in Equation (17).

$$C_{\mathrm{hess,norm}} = \frac{C_{\mathrm{hess}} - C_{\mathrm{hess,min}}}{C_{\mathrm{hess,max}} - C_{\mathrm{hess,min}}} \tag{17}$$

$C_{\mathrm{hess,min}}$ is the reference minimum value of C_{hess}. $C_{\mathrm{hess,max}}$ is the reference maximum value of C_{hess}.

The optimization constraints parameters are shown in Table 6. m_{veh} is the weight of the HESS EV.

Table 6. The optimization constraints parameters.

Parameters	Value
t_{100}(s)	<10
$V_{\mathrm{veh,max}}$/(kmph)	>100
l/(km)	>100
m_{veh}/(kg)	<1600

The weights w_1, w_2, w_3, w_4, and w_5 are chosen to indicate the importance of the five objectives. The sum of w_1, w_2, w_3, w_4, and w_5 is 1.

4. Optimization Results

The GA algorithm has been shown to be an effective strategy to solve complex and nonlinear engineering optimization problems. The GA algorithm is written in the ADVISOR software in the MATLAB environment. The GA algorithm parameters are as in Table 7.

Table 7. GA algorithm parameters.

Parameters	Value
Number of termination evolution generations	40
Crossover probability	0.95
Mutation probability	0.08

The HESS optimization flowchart diagram based on the ADVISOR software and GA algorithm is as in Figure 4. The optimized variables k_{bt}, $N_{\mathrm{bt,s}}$, $N_{\mathrm{sc,s}}$, $N_{\mathrm{sc,p}}$, and P_{charge} are encoded by binary method. w_1, w_2, w_3, w_4, and w_5 are 0.2, 0.2, 0.2, 0.2, and 0.2, respectively. The equivalent fuel economy of the HESS EV under UDDS driving condition is good. Therefore, two consecutive UDDS (Urban Dynamometer Driving Schedule) drive cycles are used in the simulation.

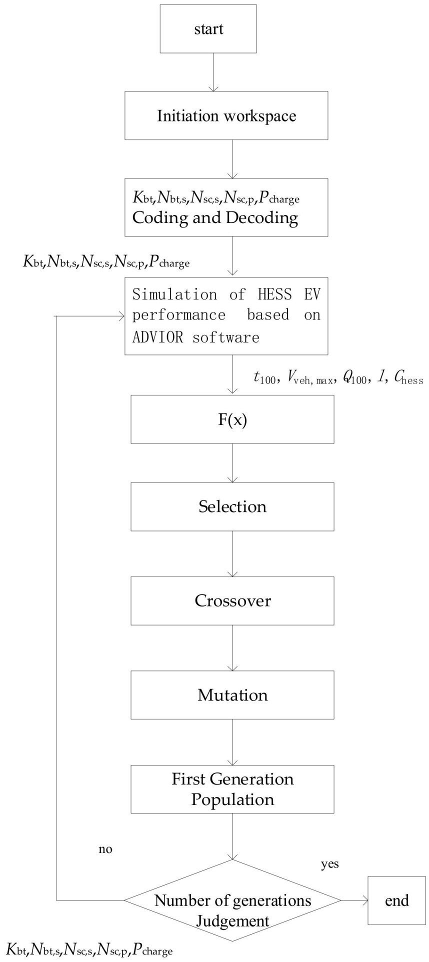

Figure 4. The flowchart diagram of the HESS optimization.

The HESS cost is evaluated by considering a BACP3000 super-capacitor cost as USD 50 and a SAFT VL45E Li-ion *BT* cost as USD 40. The Li-ion *BT* packs are replaced once in the cycle lifetime, so the cost of a *BT* is USD 80. C_{hess} is presented as Equation (18).

$$C_{hess} = 80 \cdot k_{bt} \cdot N_{bts} + 50 \cdot k_{sc} \cdot N_{scs} \cdot N_{scp} \tag{18}$$

The objection function F(x) convergence process is as in Figure 5, basically stable after nearly 15 generations.

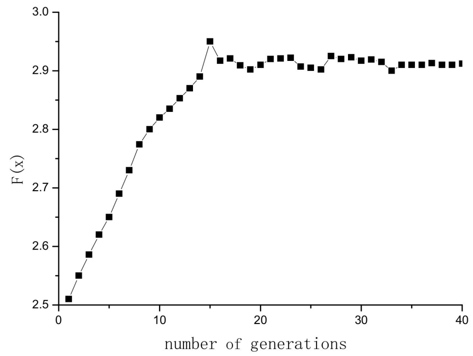

Figure 5. Objective function F(x) convergence process.

The t_{100} convergence process is as in Figure 6, basically stable after near 20 generations.

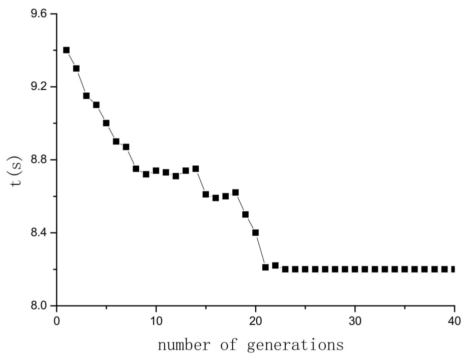

Figure 6. t_{100} convergence process.

The $V_{\mathrm{veh,max}}$ convergence process is as in Figure 7, basically stable after near 25 generations.

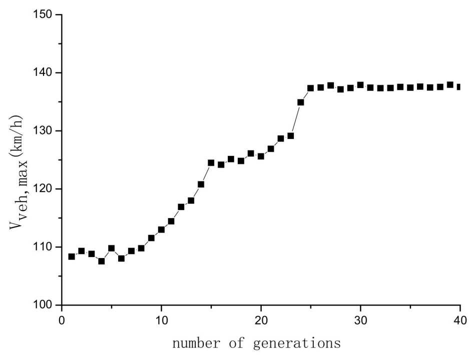

Figure 7. $V_{\mathrm{veh,max}}$ convergence process.

The Q_{100} convergence process is as in Figure 8, basically stable after near 25 generations.

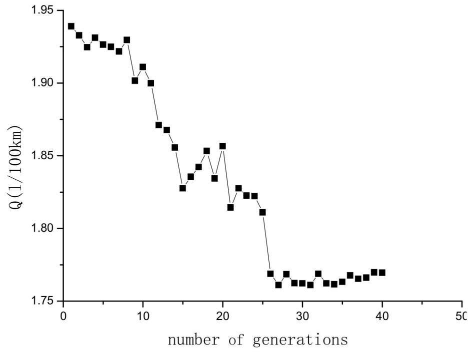

Figure 8. Q_{100} convergence process.

The C_{hess} convergence process is as in Figure 9, basically stable after near 30 generations.

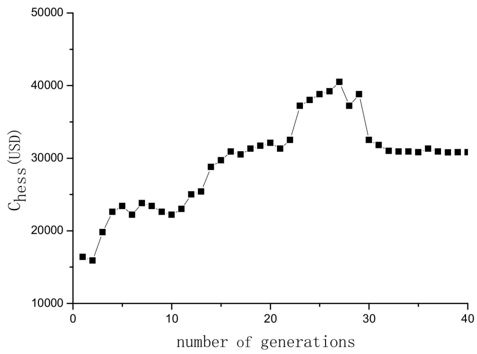

Figure 9. C_{hess} convergence process.

The l convergence process is as in Figure 10, basically stable after near 30 generations.

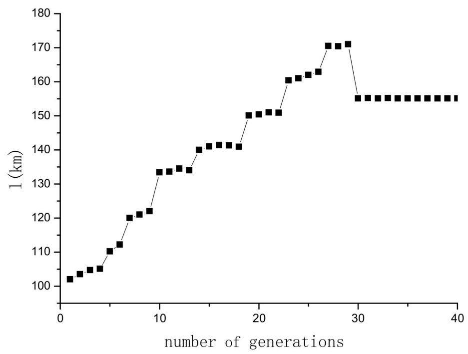

Figure 10. l convergence process.

The simulation results are as in Table 8. It is clear that the optimization results meet the constraints of the optimization. The GA algorithm can find the optimal value. The optimization results are reasonable taking into account the five objectives, such as t_{100}, $V_{\text{veh,max}}$, l, Q_{100}, and C_{hess}.

Two sets of weights are used to study their influences on the results of multiobjective optimization. The two sets of weights are as in Table 9. The five weights of the five objectives are the same in the first set of weights. This means that these five objectives are equally important. In the second set of weights, w_1, w_2, and w_5 change, but w_3 and w_4 remain unchanged comparing the first set of weights. The results are shown in Table 10. It can be seen from Tables 9 and 10 that when w_1 decreases from 0.2 to 0.15, the corresponding objective t_{100} increases from 8.2 to 9.5. When w_2 decreases from 0.2 to 0.15, the corresponding objective $V_{\text{veh,max}}$ decreases from 133.28 to 108.85. When w_5 increases from 0.2 to 0.3, the corresponding objective C_{hess} decreases from 30,800 to 19,800. Some of the multi objectives are sensitive to their weights. The weight of each objective can be selected according to the importance of each objective.

Table 8. Simulation results.

Generation Number	k_{bt}	$N_{\text{bt,s}}$	$N_{\text{sc,s}}$	$N_{\text{sc,p}}$	P_{charge}/W	t_{100}/s	$V_{\text{veh,max}}$	l/km	C_{hess} (USD)	Q_{100}/(L/100 km)
1	1.59	91	104	1	5015	9.4	108.32	102	16,400	1.9391
5	1.68	93	130	1	6500	9	109.76	110.2	23,400	1.9265
20	1.94	109	114	4	7600	8.4	125.6	150.4	32,100	1.8566
40	2.01	111.2	109	4	8100	8.2	137.5	155.1	30,800	1.7695

Table 9. Two sets of weights.

No.	W_1	W_2	W_3	W_4	W_5
1	0.2	0.2	0.2	0.2	0.2
2	0.15	0.15	0.2	0.2	0.3

Table 10. The results with two sets of weights.

No.	k_{bt}	$N_{\text{bt,s}}$	$N_{\text{sc,s}}$	$N_{\text{sc,p}}$	P_{charge} (W)	$t_{100(8)}$	$V_{\text{veh,max}}$ (km/h)	L (km)	C_{hess} ($)	Q_{100} (L)
1	2.01	111.2	109	4	8100	8.2	155.1	151.8	30800	1.7695
2	2	110.9	109.1	2	8061	9.5	108.85	154.9	19800	1.7708

The optimization of HESS EV in ADVISOR software is realized by the direct optimization algorithm, which directly uses a large number of simulations and compares the results, so as to obtain the optimal solution or approximate optimal solutions. Compared with GA algorithm optimization, the direct optimization algorithm of the HESS EV takes longer time, but the optimization effect is poor, and it is difficult to find a better solution. Compared with direct optimization algorithm, the GA algorithm has a stronger optimization ability, and the single objective is more sensitive to its corresponding weight.

5. Conclusions

Due to the nonlinear and strong coupling relationship between *BT* and SC HESS EV sizing parameters and control strategy parameters and the EV's performances, driving range, and price, as well as the different preferences of different consumers, the GA algorithm is used to study the multiobjective optimization of an HESS EV. A Li-ion semi-active HESS and optimal energy control strategy were presented for the EVs. A multiobjective optimization problem is analyzed based on the ADVISOR software in the MATLAB environment. The multi objectives include energy consumption over 100 km, acceleration time from 0–100 km per hour, maximum speed, running range, and HESS cost of an EV, and the ADVISOR software is used to obtain them. The scaled factors of *BT* capacity, the series number of Li-ion *BT*s, the series number of SCs, the parallel number of SCs, and charge power of the SCs are chosen as optimization variables. The optimization results show that the weights are sensitive to their objectives. The proposed optimization method is practical for a Li-ion *BT* and SC HESS EV.

Author Contributions: Conceptualization, G.X., Q.C., P.X., L.Z. and Q.R.; methodology, G.X. and P.X.; software, G.X., Q.C. and P.X.; validation, L.Z. and Q.R.; formal analysis, G.X. and P.X.; investigation, G.X. and Q.C.; resources, P.X.; data curation, G.X. and P.X.; writing—original draft preparation,

G.X., Q.C. and P.X.; writing—review and editing, P.X.; visualization, G.X.; supervision, Q.R.; project administration, G.X.; funding acquisition, P.X. All authors have read and agreed to the published version of the manuscript.

Funding: This research was funded by the Fundamental Research Funds for the Central Universities grant number WUT:2020IVA031 and the APC was funded by the Fundamental Research Funds for the Central Universities grant number WUT:2020IVA031.

Institutional Review Board Statement: Not applicable.

Informed Consent Statement: Not applicable.

Data Availability Statement: Not applicable.

Conflicts of Interest: The authors declare no conflict of interest.

References

1. Xu, H.; Shen, M. The control of lithium-ion batteries and supercapacitors in hybrid energy storage systems for electric vehicles: A review. *Int. J. Energy Res.* **2021**, *45*, 20524–20544. [CrossRef]
2. Wieczorek, M.; Lewandowski, M.; Jefimowski, W. Cost comparison of different configurations of a hybrid energy storage system with battery-only and supercapacitor-only storage in an electric city bus. *Bull. Pol. Acad. Sci.-Tech. Sci.* **2019**, *67*, 1095–1106.
3. Wang, Z.; Deng, Z.H.; Zhu, R.J.; Zhou, Y.H.; Li, X. Modeling and analysis of pumping cell of NOx sensor–Part I: Main oxygen pumping cell. *Sens. Actuators B Chem.* **2022**, *359*, 131622. [CrossRef]
4. Xia, Z.; Deng, Z.; Jiang, C.; Zhao, D.Q.; Kupecki, J.; Wu, X.L.; Li, X. Modeling and analysis of cross-flow solid oxide electrolysis cell with oxygen electrode/electrolyte interface oxygen pressure characteristics for hydrogen production. *J. Power Sources* **2022**, *529*, 231248. [CrossRef]
5. Tian, Y.; Huang, Z.; Long, T.; Tian, J.; Li, X. Performance analysis and modeling of three energy storage devices for electric vehicle applications over a wide temperature range. *Electrochim. Acta* **2020**, *331*, 135317. [CrossRef]
6. Liu, G.; Zhao, W.; Li, Z.; Xia, Z.; Jiang, C.; Kupecki, J.; Li, X. Modeling and control-oriented thermal safety analysis for mode switching process of reversible solid oxide cell system. *Energy Convers. Manag.* **2022**, *255*, 115318. [CrossRef]
7. Zhang, Q.; Li, G. Experimental Study on a Semi-Active Battery-Supercapacitor Hybrid Energy Storage System for Electric Vehicle Application. *IEEE Trans. Power Electron.* **2020**, *35*, 1014–1021. [CrossRef]
8. Kouchachvili, L.; Yaici, W.; Entchev, E. Hybrid battery/supercapacitor energy storage system for the electric vehicles. *J. Power Sources* **2018**, *374*, 237–248. [CrossRef]
9. Kim, J.; Shin, D.; Baek, D.; Park, J.D. Optimization of Supercapacitor Hybrid Architecture for Power Supply-Connected Batteries Lifetime Enhancement. *Electronics* **2019**, *8*, 41. [CrossRef]
10. Lencwe, M.J.; Chowdhury, S.P.; Olwal, T.O. A Multi-Stage Approach to a Hybrid Lead Acid Battery and Supercapacitor System for Transport Vehicles. *Energies* **2018**, *11*, 2888. [CrossRef]
11. Lencwe, M.J.; Chowdhury, S.P.D.; Olwal, T.O. An Effective Control for Lead-Acid Performance Enhancement in a Hybrid Battery-Supercapacitor System Used in Transport Vehicles. *Sustainability* **2021**, *13*, 13971. [CrossRef]
12. Łebkowski, A. Studies of Energy Consumption by a City Bus Powered by a Hybrid Energy Storage System in Variable Road Conditions. *Energies* **2019**, *12*, 951. [CrossRef]
13. Cao, J.; Du, W.; Wang, H.; McCulloch, M. Optimal Sizing and Control Strategies for Hybrid Storage System as Limited by Grid Frequency Deviations. *IEEE Trans. Power Syst.* **2018**, *33*, 5486–5495. [CrossRef]
14. Dao, H.V.; To, X.D.; Truong, H.V.A.; Do, T.C.; Ho, C.M.; Dang, T.D.; Ahn, K.K. Optimization-Based Fuzzy Energy Management Strategy for PEM Fuel Cell/Battery/Supercapacitor Hybrid Construction Excavator. *Int. J. Precis. Eng. Manuf.-Green* **2021**, *8*, 1267–1285. [CrossRef]
15. Lukas, K.; Astrid, B.; Richard, H.-R. Optimal Design of Power Gradient Limited Solid Oxide Fuel Cell Systems with Hybrid Storage Support for Ship Applications. *Energy Convers. Manag.* **2021**, *243*, 114396.
16. Wang, Y.; Sun, Z.; Chen, Z. Energy management strategy for battery/supercapacitor/fuel cell hybrid source vehicles based on finite state machine. *Appl. Energy* **2019**, *254*, 113707. [CrossRef]
17. Yang, B.; Wang, J.; Zhang, X.; Wang, J.; Shu, H.; Li, S.; He, T.; Lan, C.; Yu, T. Applications of battery/supercapacitor hybrid energy storage systems for electric vehicles using perturbation observer based robust control. *J. Power Sources* **2020**, *448*, 227444. [CrossRef]
18. Zhang, Q.; Wang, L.; Li, G.; Liu, Y. A real-time energy management control strategy for battery and supercapacitor hybrid energy storage systems of pure electric vehicles. *J. Energy Storage* **2020**, *31*, 101721. [CrossRef]
19. Zhang, C.; Wang, D.; Wang, B.; Tong, F. Battery Degradation Minimization-Oriented Hybrid Energy Storage System for Electric Vehicles. *Energies* **2020**, *13*, 246. [CrossRef]
20. Liu, H.; Xing, X.; Shang, W.; Li, T. NSGA-II Optimized Multiobjective Predictive Energy Management for Fuel Cell/Battery/Supercapacitor Hybrid Construction Vehicles. *Int. J. Electrochem. Sci.* **2021**, *16*, 21046. [CrossRef]

21. Mao, Y.; Niu, S.X.; Yang, Y. Differential Evolution-Based Multiobjective Optimization of the Electrical Continuously Variable Transmission System. *IEEE Trans. Ind. Electron.* **2018**, *3*, 2080–2089. [CrossRef]
22. Battapothula, G.; Yammani, C.; Maheswarapu, S. Multi-objective simultaneous optimal planning of electrical vehicle fast charging stations and DGs in distribution system. *J. Mod. Power Syst. Clean Energy* **2019**, *4*, 923–934. [CrossRef]
23. Akbari, M.; Brenna, M.; Longo, M. Optimal Locating of Electric Vehicle Charging Stations by Application of Genetic Algorithm. *Sustainability* **2018**, *4*, 1076. [CrossRef]
24. Ma, C.R.; Mao, B.H.; Zhang, T. Multi-Depot Vehicle Routing Optimization Considering Energy Consumption for Hazardous Materials Transportation. *Sustainability* **2018**, *10*, 3519. [CrossRef]
25. Peng, X.; Shuhai, Q.; Changjun, X. Simulation of a Li-ion battery/supercapacitor hybrid system for electric vehicle based on secondary development of ADVISOR. In Proceedings of the 2017 First International Conference on Electronics Instrumentation & Information Systems (EIIS), Harbin, China, 3–5 June 2017; pp. 1–5.
26. Peng, X. Study on Modeling, Energy Control Strategy and performance of Hybrid Power System for Electric Vehicle. Doctoral Dissertation, Wuhan University of Technology, Wuhan, China, 2018; p. 5.